The materials for the National Report on the results of fundamental space research in Russia in 2010-2011
D.V. Skobeltsyn Institute of Nuclear Physics
M.V. Lomonosov Moscow State University

The objective of the scientific research of the Institute's team is to obtain breakthrough knowledge and quantitative information about the fundamental laws which control interrelated dynamics of space radiation and electromagnetic processes on the Sun, in the heliosphere and in the Earth's magnetosphere. Experimental and theoretical studies are aimed at the development of the practically important physical basis for monitoring of the near-Earth space conditions and for the clarification of the mechanisms of the influence of space radiation factors on space and ground-based systems under the conditions of changing solar activity. Space experiments and intensive theoretical studies accompanied by mathematical simulation and development of the modern storage systems for space monitoring data are conducted. During 2010-2011 the main subjects of the studies included the following directions of the solar-terrestrial physics: studies of radiation conditions both in the interplanetary and in the near-Earth space during the solar activity cycle including 2010 and 2011 – the period of solar activity increasing after the prolonged solar activity minimum.

I. *Development of scientific equipment for radiation measurements onboard satellites.*

In 2010-2011 the following satellites with scientific equipment developed by the SINP scientists were successfully launched:

- Nine satellites of the GLONASS series (circular orbit with altitude of 20 thousands km) with dose radiometer (RD) which monitors the near-Earth space (beginning from 2005 there are 29 satellites of the GLONASS series with RD onboard are operated);

- Sun-synchronous satellite "Meteor-M1" (polar orbit with altitude of ~830 km) with the instruments MSGI-MKA and SKL-M intended for registration of electron flux with energy from ~100 keV up to ~20 MeV and protons with energy from ~1 up to ~300 MeV;

- Geostationary satellite "Elektro-L" (altitude ~36000 km, longitude — 76°) with spectrometer SKL-E intended for registration of electrons of the Earth's radiation belt and protons of the Earth's radiation belt and solar flares;

- Russian-Indian University satellite "YouthSat" (sun-synchronous circular orbit with altitude of about 800 km) with the instruments SOLRAD intended for registration of hard radiation (gamma-radiation with E=0.02-5.0 MeV) and charged particles of the solar flares (electrons with E=0.1-4.0 MeV and protons with E=2-80 MeV). Detection block is directed to the Sun.

- Microsatellite of IKI RAS "Chibis-M" (circular orbit with altitude of ~500 km and inclination of 51°) with detectors RGD (X-rays and gamma-radiation within the energy ranges of 0.2-2.0 MeV) and DUV (UV (300-400 nm) and red (600-700 nm) radiation) intended for registration of atmospheric bursts of optical, UV, X-rays and gamma-radiation associated with lightning discharges.

Radiation fields of the Earth's magnetosphere were experimentally studied by means of the scientific equipment onboard the mentioned satellites and the system of radiation control operated onboard the International Space Station (system of semiconductor dosimeters DB-8). Great volume of experimental space-physical information was obtained. Development of scientific equipment complexes for the studies of radiation in the near-Earth space was continued.

Proposed experiments

MSU Project "Lomonosov"

MSU started a new scientific-educational project "Lomonosov". Moscow state university is named after M.V. Lomonosov, whose 300th anniversary was celebrated in 2011. Name of M.V. Lomonosov onboard the satellite is a tribute to the memory and respect to the outstanding Russian scientist who did a lot for the foundation of MSU, besides scientific problems which he raised are close to the scientific goals of the "Lomonosov" project.

The launch of the "Lomonosov" satellite will be the third within the frames of the space scientific-educational program "MSU-250" which provides development of non-expensive space platform for the experiments in space by University scientists, educators and students. Launches of "Univeristetsky-Tatiana" (2005) and "Universitetsky-Tatiana-2" (2009) satellites had their continuation in the solution of many actual problems of space science and education in MSU.

The purpose of the development of the spacecraft "Lomonosov" is to conduct fundamental research in the field of cosmic rays physics, astrophysics and physics of magnetosphere.

Spacecraft (SC) "Lomonosov" was based on a platform "Kanopus-V", developed by the Research and Production Corporation "Space-Monitoring Systems, Information and Control and Electromechanical Complexes" named after A.G. Iosifian (VNIIEM). SC will be launched to the circular sun-synchronous orbit with an altitude of 550 km. The mass of the scientific instrument module is about 240 kg from 550 kg of the total mass of the SC.

The project provides the following scientific equipment (SE) onboard the SC:

The studies of the cosmic rays of extremely high energy (10^{19} -10^{20} eV) in the area of the energy spectrum cutting "GZK-cutting off", which was predicted by Greisen, Zatsepin and Kuzmin (SE TUS).

The instrument TUS provides registration of UV radiation of EAS caused by the space radiation with energy $E > 5 \times 10^{19}$ eV. The instrument consists of a mirror-concentrator with diameter of about 2 meters, in the focus of which a receiver of UV radiation – mosaic of 256 photomultipliers is situated. Additionally to the studies of the particles of extremely high energy TUS provides the studies of fast light events in the upper atmosphere, started by the previous space projects of the MSU "Universitetsky-Tatiana" and "Universitetsky-Tatiana-2". Information volume of the TUS instrument is 200 Mbytes/day.

The studies of the space gamma-bursts – the most energetic processes in the Universe within the optical (SE ShOK-1), UV and X-ray (SE UFFO) and gamma-ranges of the wavelengths (SE BDRG 1-3).

Complex of the instruments ShOK, BDRG and UFFO provides multiwave measurements of gamma-bursts which are necessary for the studies of the nature of these astrophysical sources. SE BDRG consists of three detectors of gamma-radiation which register gamma-quanta with energy of 0,03-10 MeV. SE ShoK consists of two immobile fast wide-angle cameras, which photograph star sky. The frames synchronized by time with appearance of the signal of the SE BDRG are transmitted to the ground-based information collection point. SE UFFO consists of 20-cm mirror with a receiver sensitive within the range of 200-650 nm wavelengths and X-ray detector which registers quanta with energy of 5-200 keV. SE UFFO is operated according to the control signals

from X-ray detector and SE BDRG. Information volume of multiwave complex of gamma-bursts is 3 Gbytes/day.

The studies of the magentospheric particles – possible sources of transient and quasi-stationary phenomena in the upper atmosphere (SE ELFIN-L and SE DEPRON).

SE DEPRON is intended for the measurements of the absorbed doses and spectra of linear energy transfer (LET) from high-energy electrons, protons and nuclei of space radiation, and for registration of thermal and slow neutrons. SE ALFIN-L is intended for the studies of physical processes responsible for the dynamics of the near-Earth radiation medium. Information volume of the magnetospheric complex is about 20 Mbytes/day.

Actual applied research such as approbation of the space autotrack of the small celestial bodies, asteroids and spacecrafts (SE ShOK), experiment on optimization of the onboard navigation system SE IMISS-1) will be also conducted onboard the SC.

During the orbital flight the SC is situated in the orbital orientation, beginning of which is rigidly connected with the center of masses of the SC: «+X» axis is directed along the vector of orbital speed and lays in the plane of the orbit; «+Z» axes is directed along the radius-vector connecting the center of the Earth with the center of the masses of the SC and looks to the zenith; «+Y» axes is perpendicular to the orbital plane and elaborates the system of coordinates to the right one. In the Figure 1 the position of the SC during the orbital flight is presented. In the Figure 2 location of the instruments and their fields of view are presented.
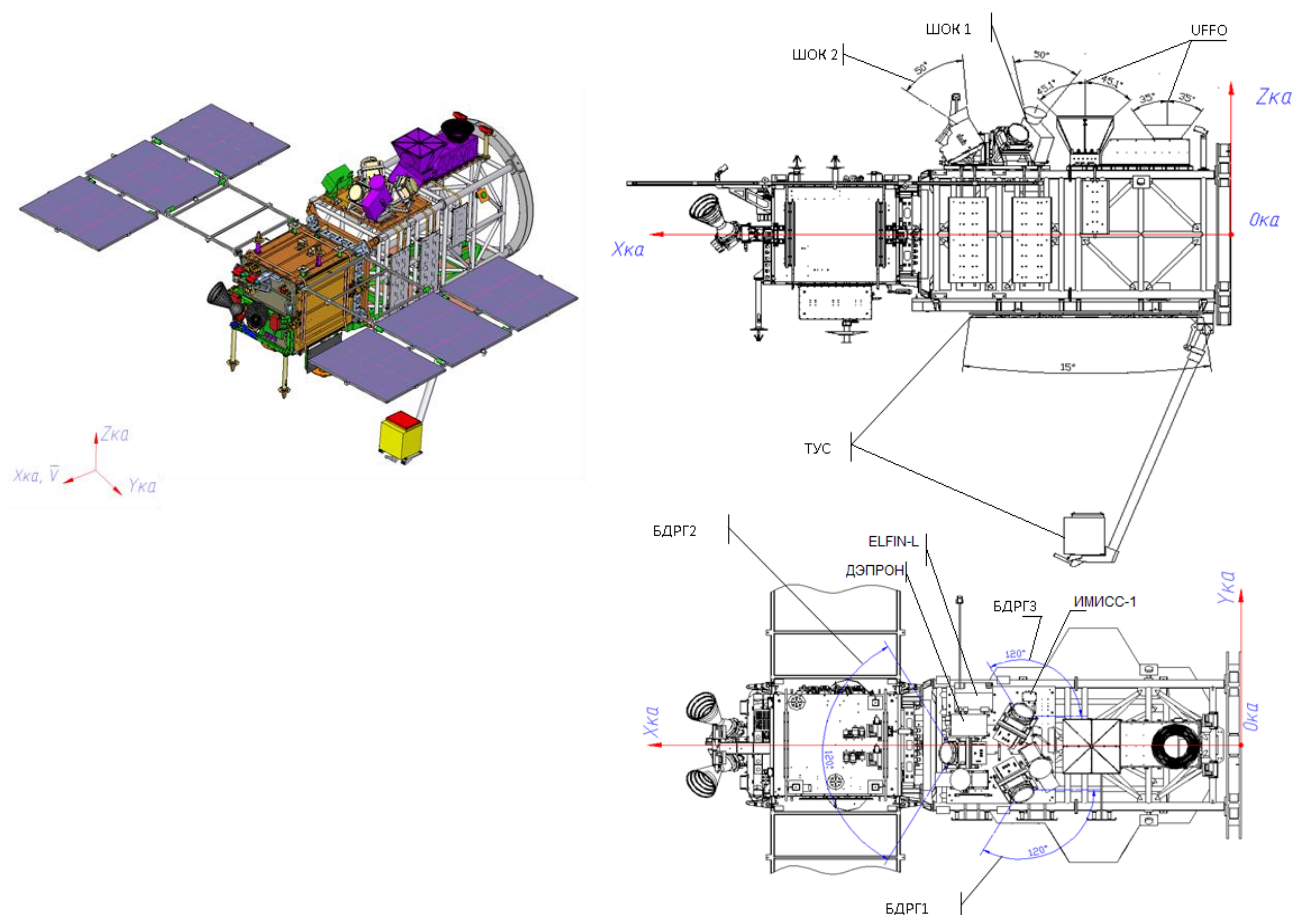

Fig.1. «Lomonosov» SC during the orbital flight.

Fig.2. "Lomoosov" SC: location of the instruments and their fields of view.

Space experiment NUCLEON

The goal of the experiment NUCLEON is to measure energy spectra with elementwise resolution of cosmic rays components within the range of 10^{11}-10^{15} eV by means of superlight instrument during a long-term orbital flight as a supplementary payload onboard the Russian serial spacecraft.

The basic concept of the NUCLEON experiment is development of relatively light (about 300 kg) and size (less than 1.0 m^3) SE, which can solve actual problems of the experimental physics of cosmic rays within the wide energy range 10^{11}-10^{15} eV. This approach does not require own instrument carrier, as it was during the previous research. It can be exposed by means of the additional reserves which regularly appear onboard serial Russian SCs during the long-term tasks execution. Such conception allows to minimize expenses and bring closer the date of space experiment as close as possible.

Tactical and technical characteristics of the scientific equipment

- Complex of scientific equipment (CSE) NUCLEON must provide registration of cosmic rays of high energy within the energy range from 10^{12} to 10^{15} eV and within the range of charges Z=1-30, effective geometry factor of CSE NUCLEON must be about 0.30 m^2sr, for all types of CR particles.

- CSE NUCLEON must provide elementwise resolution of CR nuclei, average error for the charge measurements must be not over 0.3 charge unit.

- CSE NUCLEON must provide measurements of the primary particle energy. Average error is energy measurements must be not over 80% for individual event within the specified range of CR nuclei.

- CSE NUCLEON must separate the events for registration of CR particles with first non-elastic nuclear interaction in the target matter. In the trigger system CSE must provide possibility for the measurements of energy threshold of registration of CR primary particles. Time of trigger signal production for information reading from the CSE detectors must be less than 1 mks.

- In the aperture of not less than 0.1 m^2sr — CSE NUCLEON must provide separation of electromagnetic component (electrons, positrons, gammas) from the CR composition. The level of rejection of CR nuclei into MIK must be not less than 10^{-4}. Average error of energy measurements must be less than 12% for individual event of electromagnetic component.

The main technical characteristics of the scientific equipment

- Mass of SE is ~300 mg, in the pressurized container less than 360 kg;

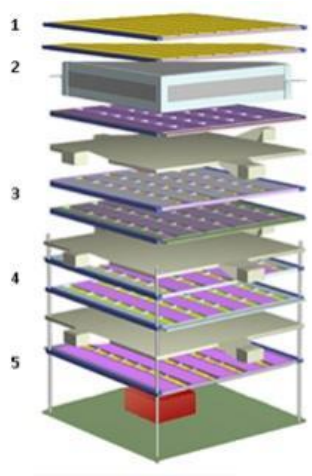- Energy consumption of SE <160 W;

- Daily telemetry volume ~10 GBytes;

- Number of independent sensors of the SE – 11104;

1. Warranty operation period ≥5 years.

Mechanical construction of SE assembled is a monoblock of "layered" structure with size of the active part of spectrometer ~500x500x360 mm^3. A scheme of the layers position is presented in Figure 1.

Totally there are 14 layers. Sequence of the layers in the direction from zenith to nadir is the following:

- 1 and 2 layers compose a system of charge measuring;

- 3, 4, 6,7,9,10,12 layers compose a system of energy measuring;

- 5, 8,11 layers compose a scintillation system of fast trigger;

- 13 layer is a micro ionization calorimeter;

- 14 layer is a block of supporting electronics.

Figure 1.

Location of CSE NUCLEON onboard the serial SC

CSE NUCLEON is located in a pressurized container (PC) which equipped with a system of thermal regulation and system of telemetry sensors which control medium parameters in PC (Figure 2).

Figure 2

Operation of CSE NUCLEON is planned as supplementary payload for the SC "Resurs-P" N2 (Figure 3).

Figure 3

Comparative characteristics of the NUCLEON instrument and the current foreign experiments on the research of proton-nuclear and electron components of high-energy cosmic rays

Table 1 a. Protons and nuclei

Experiment	Γ m^{2}sr	t, Exposure time	Γt m^{2}sr year	Energy resolution, %
NUCLEON with micro calorimeter	~0.3	5 years	2/0.75 0.65/0.15	~70-80 ~40-50
Fermi-LAT (GLAST) (only protons)	~0.5	5 years	~2.5	~50 (?)
AMS02	0.5	10 years	5	Energy threshold at ~10^{13} eV
CREAM	1.3/0.46 nuclei/protons	Up to 0.5 year	0.65/0.23	50
CALET	~0.4/0.15 nuclei/protons	3 years	~1.2/0.45	~50 (?)
PAMELA	0.00216	>3	0.0065	>40
ATIC	0.25/0.15 nuclei/protons	~0.2-0.3 years for all flights	~0.006/0.0034	~30

Table 1 b. Electrons

Experiment	Γ m^{2}sr	t, Exposure time	Γt m^{2}sr year	Energy resolution, %
NUCLEON with micro calorimeter	0.13	5 years	0.65	5
NUCLEON with a big calorimeter	0.66	5 years	3.3	5
Fermi-LAT (GLAST)	2.8-1 (100-1000 GeV)	5 years	14-5	12/33
AMS02	0.5	10 years	5	~20 (depends on energy)
CALET	~1	3 years	3	~3
PAMELA	0.00216	>3	0.0065	5.5
ATIC	0.25	~0.2-0.3 years for all flights	~0.006/0.0034	3

The presented data allows to make the following conclusions: according to the parameters CSE NUCLEON is an instrument of the following generation (compared with the experiments PAMELA and ATIC) and at the front line of the world level taking into account generality of the measurements and expected volume of statistical material.

Space experiment RELEC

The goal of the experiment RELEC (relativistic electrons) is to study mechanisms of acceleration and precipitation of magnetospheric relativistic electrons and their possible influence on the upper atmosphere of the Earth. Within the frames of the experiment it is also planned to study high-altitude electric discharges within the wide range of electromagnetic spectrum; it is supposed to measure intensity of electromagnetic radiation of high-altitude discharges within radio, optical, UV, X-ray and gamma-ranges. The experiment must be conducted onboard a small spacecraft of MKA-FKI series developed by the scientific and production center named after S.A. Lavochkin. The launch of the satellite is planned for 2013.

SE includes the following instruments: two identical detectors of X-ray and gamma-radiation DRGE-1 and DRGE-2, detector of electrons DRGE-3, detector of UV and red radiation DUV, optical and UV telescope "Telescope-T", analyzer of low-frequency radiation NchA, analyzer of high-frequency radiation RchA, dozimetry instrument Dostel, block of electronics BE.

Characteristics of the instruments:

DRGE-1 (DRGE-2) instrument:
- energy range of registered gamma-quanta $0.01 - 3.0$ MeV;
- total effective area of all detectors ~ 500 cm^2;
- time resolution 10 mks;
- sensitivity (minimum registered flux) $- 10^{-7}$ erg/cm^2;
- mass $- 10$ kg (1 block);
- energy consumption 8 W (1 block);
- information volume 200 MBytes/day.

DRGE-3 instrument:
- energy range of registered electrons 0.4 – 10.0 MeV;
- effective area of detectors ~3 cm^2;
- time resolution 10 mks;
- dynamic range – 1-10^4 cm^{-2}/s^{-1};
- mass – 3 kg;
- energy consumption 9 W;
- information volume 100 MBytes/day.

DUV instrument:
- wavelength range of registered photons 300-400, 600-700 nm;
- time resolution 500 mks;
- mass – 0.7 kg;
- energy consumption 2.5 W;
- information volume 10 MBytes/day.

«Telescope-T» instrument:
- wavelength range of registered photons 200-600 nm;
- spatial resolution from the altitude of 800 km 2x2 km^2;
- time resolution 100 mks;
- mass – 4 kg;
- energy consumption 6 W;
- information volume 200 MBytes/day.

NChA instrument:
- frequency range 0.1 Hz – 40 kHz;
- number of analyzed components of electric and magnetic field - 3;
- number of channels of spectral analyzer – 256;
- total mass of all blocks 2.5 kg;
- energy consumption 5.5 W;
- information volume 300 MBytes/day.

RChA instrument:
- frequency range 50 kHz – 15 MHz;
1. number of analyzed components of electric and magnetic field - 3;
2. spectral resolution ~0.1-2.0%;
3. time resolution 25 ns;
4. dynamic range 80 dB;
- total mass of all blocks 1.5 kg;
- energy consumption 10 W;
- information volume 200 MBytes/day.

Dostel instrument:
- spectral range of linear losses of energy0.1-200 keV/mkm;
- effective area of the detectors 6.93/1.0 cm^2;
- mass – 1.2 kg;
- energy consumption 3 W;
- information volume 3 MBytes/day;

BE instrument:
- mass – 2.1 kg;
- energy consumption 5 W;
- transmitted information volume – up to 1 GBytes/day.

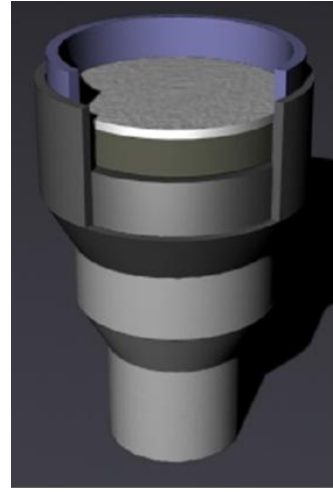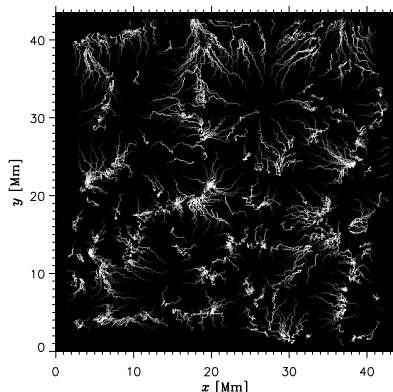Fig. Layout of the instruments of the SE RELEC.

Fig. Layout of the block of X-rays, gamma-radiation and high-energy electron detectors for the RELEC experiment.

Panasyuk M.I., Bogomolov V.V., Garipov G.K. et al. Transient Luminous Event Phenomena and Energetic Particleы Impacting the Upper Atmosphere: Russian Space Experiment Programs // Journal Geophys. Res. 2010. V.115, A00E33, doi: 10.1029/2009JA014763, p.1-5.

II. *Studies of dynamical processes on the Sun and in heliosphere*

About the structure of the convective rates field in the photosphere of the Sun

The studies of the behavior of horizontal rates field in the photosphere of the Sun with averaging through different time intervals found out "big mesograins" with size of about 15 Mm. The areas of strong convergence of horizontal flows which sometimes is accompanied by twisting are found out. Probably there are convective cells with differently directed matter's circulation – so-called *l-* and *g*-types.

Fig. Trajectories of the imaginary sample particles during the two-hours interval. In the right upper part of the Figure a "big mesograin" imposed on the supergrain is seen, in the lower part – mesograins of ordinary size. In many cases "big mesograins" are star-shaped.

A.V. Getling, A.A. Buchnev About the structure of the convective rates field in the photosphere of the Sun // Astronom. J., V.87, N3, pp. 286-292, 2010.

To the question about the general magnetic field of the Sun

By means of numerical simulation of the cellular convective flows in the polytropic stratificated rotating layer of the compressible media the relations between the average helicity of the rates field (h), polytrope's index (m) and the layer's rotation rate (Ω) is studied. In the theory of turbulent MGD dynamo average helicity is an important parameter of large-scale magnetic field generation (in particular, general magnetic field of the Sun) which is responsible for so-called α-effect. If we assume that the rates field is turbulent than the value of helicity depends strongly on the hypothesis of the turbulence properties and therefore significant arbitrariness is inevitable. The conducted studies have shown that numerical simulation of "determinated" relatively stable convective flows can provide higher certainty to the estimation of helicity.

Fig. Average helicity $\langle h \rangle = \mathbf{v} \cdot \mathrm{rot}\ \mathbf{v}$ of the cellular convective flow as a function of angular rotation rate of the layer Ω at different values of the polytrope's index m. It is shown that average helicity has a maximum as a function of rotation rate.

Getling A.V. Helicity of the rates field at cellular convection in the rotating layer // Astronom. J., Vol.89, N5, pp.441-448, 2012.

Correlation relationship

It is found out that the magnetic field of the Sun at the level of chromosphere in the area of coronal holes (opened force lines) with south polarity is correlated with Akasofu parameter of magnetic activity, which characterizes energetic component of the solar wind and efficiency of its interaction with the Earth's magnetosphere.
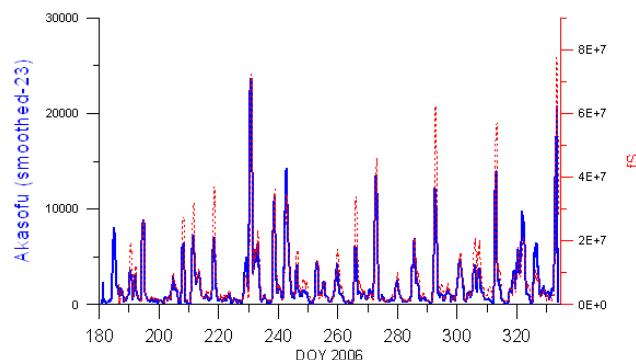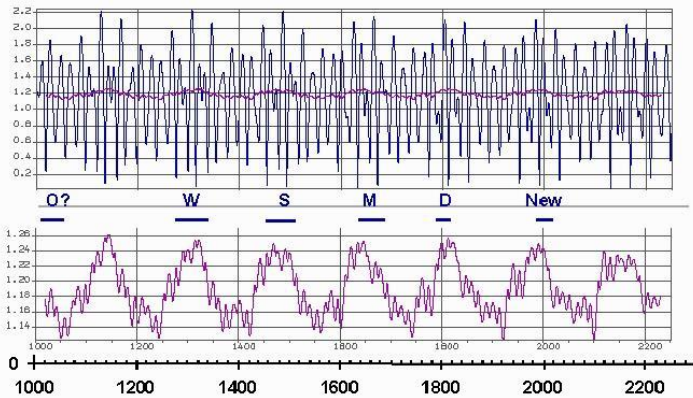

Fig. Variations of Akasofy parameter (blue solid line) and ratio of magnetic fluxes of coronal holes fN,S=Φ3000/Φ1.5 at the altitude of 3000 m and 1.5 solar radii for the vector of the opened magnetic field of the south polarity (red dashed line) for the period from July till November 2006, the last are moved to the right for 130 hours taking into account the time of solar wind flux coming.

Prosovetsky D.V., Myagkova I.N. The Correlation between Geomagnetic Disturbances and Topology of Quasi-open Structures in the Solar Magnetic Field // Geomagnetism and Aeronomy, Vol. 51, No. 8, pp. 1078–1082, 2011.

Solar activity

It was shown that the prolonged solar activity minima observed in the past during the periods when the center of the masses of the Solar system (the Sun and the external planets) situated out of the solar sphere. By means of spectral analysis of the long data-array on the number of the solar spots it was found out that there are constant spectral lines with periods close to the combination of

the rotation periods of several planets around the Sun. It was concluded that the planets influence on the process of the solar spots generation. A new paradigm of the solar activity process and solar spots generation is suggested: a falling of the celestial body (comets, asteroids) on the photosphere of the Sun is a trigger mechanism for the beginning of the solar spot generation; when the center of the masses of the Solar system is located out of the Sun, the most part of the celestial bodies does not fall on the Sun and prolonged minimum of solar activity is observed.

Fig. The distance (in solar radii) between the center of the Sun and the center of the masses of the Solar system depending on the time (the upper panel) and 40-years smoothed data (lower panel). Time intervals of prolonged solar activity minima are shown.

Okhlopkov V.P., Stozhkov Yu.I. SOLAR ACTIVITY IN PRESENT AND IN THE NEAREST FUTURE // Izv.RAN Ser.phys. 2011, vol.75, N5, pp.911-914.

Movement of the Sun relatively the center of the masses of the Solar system

Dynamic parameters of the movement of the Sun relatively the center of the masses of the Solar system – distance from the center of the Sun to the center of the masses, angular momentum of the Sun and its variation, are studied. It is shown that for the appropriate frequency interval the main period is not of 178.8 years, but period of 169 years, associated with the influence of the Neptune on the movement of the Sun. The periods associated with spectral lines observed in the Wolf numbers arrays coincide with combinations of the rotation periods of two and more planets, i.e. movement of the planets affects the solar activity.
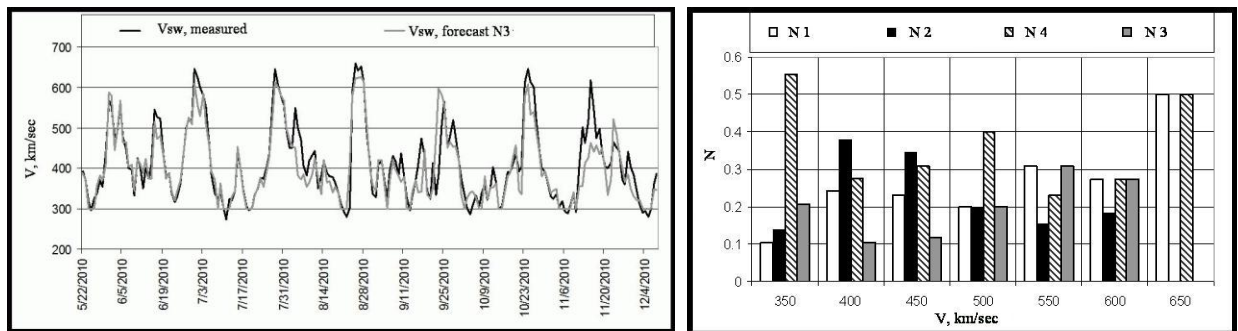

Fig.

a – time course of the distance r (in solar radii) between the center of the Sun and the center of the masses of the solar system,

b – r frequency spectrum.

Okhlopkov V.P. The main periodicities of the movement of the Sun relatively the center of the masses of the Solar system and the solar activity. Vestnik MGU. Ser.3. Phys. Astron. 2011. N6, pp.139-143

Forecasting of the quasi-stationary high-speed fluxes of the solar wind.

Hierarchical approach to the forecasting of the quasi-stationary high-speed fluxes of the solar wind (SW) allowed to merge dissimilar input data into the united system and to increase the accuracy of the SW speed forecasting. The analysis was based on the daily values of the coronal holes areas measured in 2010 by the instruments SWAP and AIA onboard the SC PROBA2 and SDO, respectively, calculated on the images of the Sun within the UV range of wavelengths and on the information about the measured SW flux speed during the previous revolutions of the Sun. At the second ranking level the SW speed for the next three days was forecasted finally. Using of this method makes the data gaps of one spacecraft not critical for the final result of the whole system forecasting.

Fig. In the left panel: black curve − daily values of the observed SW speed, gray curve 0 "forecast" of the SW speed by the committee N3 ("forecast" is an estimation of the forecasting potential by the expert system). In the right panel: histogram of the distribution of the observed SW speeds, "forecasted" by each of the experts of the committee N3 normalized to the number of the events separately for each speed range. Expert N1 − white columns, N2 − black columns, N3 − gray columns, N4 − dashed columns.

Shugay, Yu. S.; Veselovsky, I. S.; Seaton, D. B.; Berghmans, D. Hierarchical approach to forecasting recurrent solar wind streams // Solar System Research, 2011, Volume 45, Issue 6, pp.546-556.

Gamma-radiation of the solar flares

Analysis of data obtained by the SONG detector during the CORONAS-F mission for the solar flares of 25 August 2001, 28 October 2003, 4 November 2003, and 20 January 2005 has shown that the pion-produced radiation appears during the time interval of the main energy release. This can be determined as the peak times of hard X-ray bremsstrahlung and of the high-frequency radio emission at millimeters up to submillimeters wave-length. This time also corresponds to the peak of the thermal soft X-ray emission derivative recorded by GOES monitors. The onset of the pion-decay gamma-emission during the flare on 28.10.2003 coincided in time with the highest magnetic flux variation rate.
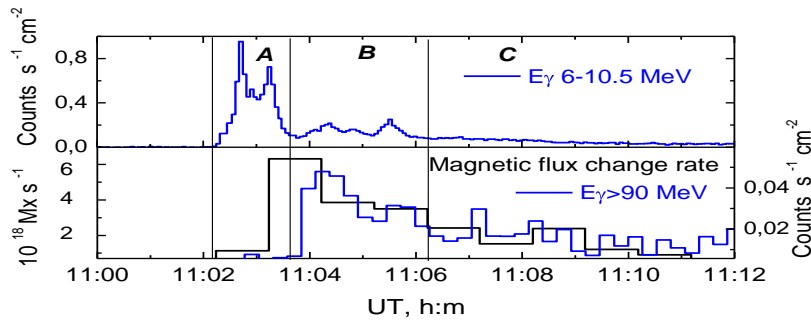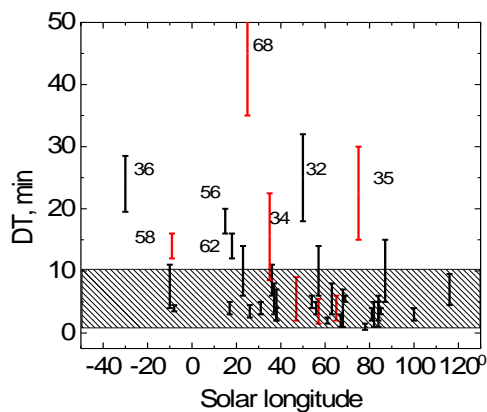
Fig. Time profiles of the gamma-ray emission measured by the SONG detector during the flare of October 28, 2003 (blue curves) and the magnetic flux variation rate (from Miclenic *et al.*, *Astron. Astrophys.,* **499**, 893, 2009 – black curve).

Kurt V.G., Yushkov B.Yu., Kudela K., Galkin V.I. High-energy gamma radiation of solar flares as an indicator of acceleration or energetic protons. Cosmic Research. 2010. V.48, P.70-79.

Kuznetsov S.N., Kurt V.G., Yushkov B.Yu., Kudela K., Galkin V.I., Gamma-Ray and High-Energy-Neutron Measurements on CORONAS-F during the Solar Flare of 28 October 2003 // Solar Physics. 2011. V.268, p. 175-193.

Acceleration of the protons in the flare

Comparison of the data recorded since 1972 by the world neutron monitor network and GOES measurements of protons with energies above 500 MeV related to 44 Ground level enhancements (GLEs) and light curves of neutral emissions of the associated flares revealed that the delay of the earliest arrival time of high-energy protons at 1 AU (T_{onset}) with respect to the observed peak time of the solar bursts (T_0) did not exceed 10 min in 30 events (see Figure 2) which corresponds to the particle propagation time. This result indicates that the efficient acceleration of protons responsible for the GLE onset in the most events has to be close to the time of the main flare energy release.
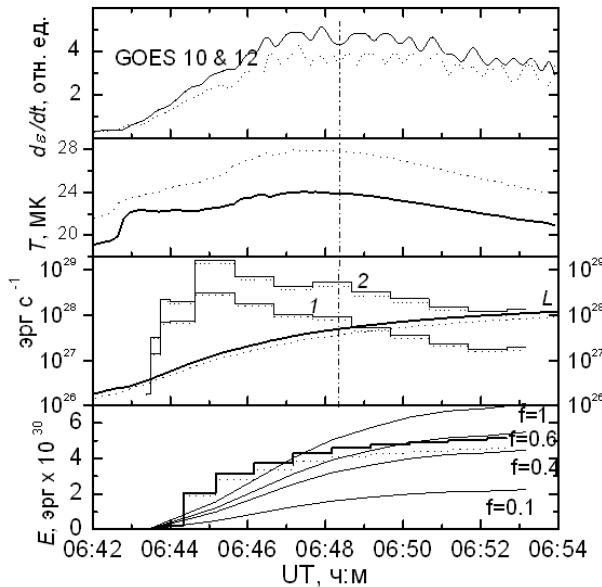

Puc. Distribution of time delay DT = T_{onset} - T_0 vs heliolongitude of associated flare.

Kurt V., Yushkov B., Belov A., Chertok I., Grechnev V. A Relation between Solar Flare Manifestations and the GLE Onset // 32nd International Cosmic Ray Conference, Beijing, 2011, paper 0441

Dynamics and energy of the solar flare

The power input by the accelerated electrons into the flare volume was evaluated for one of the most powerful solar flares of 20.01.2005 within the frames of thick target model within two assumptions about the value of the boundary energy E_0 of electron spectrum. Comparison of the

total energy, input by electrons, with thermal energy of radiating plasma has shown that at the beginning of the impulse phase of the flare total energy input by the accelerated electrons 1.5 − 2 times higher than thermal energy of plasma, then these two energies become approximately equal a the level of $\sim(4\text{-}5)\cdot10^{30}$ erg each.

Fig. Upper panel: time series of derivative of emission measure.

The second panel from the top: time series of the temperature of the heated plasma.

The third panel from the top: histogram of the energy of non-thermal component, calculated taking into account the boundary energy $E_{\gamma0}$ (1) and according to the model by Emsly (2), solid lines − time series of radiation losses.

Lower panel: histogram of the course of the input (accumulated) energy of non-thermal component; the curves show time course of thermal component energy at different values of filling coefficient (f). For all panels solid curves and histograms are based on the data of GOES-10, dashed − of GOES-12 satellite.

Kurt V.G., Svertilov S.I., Yushkov B.Yu., Bogomolov A.V., Grechnev V.V., Galkin V.I., Bogomolov V.V., Kudela K., Logachev Yu.I., Morozov O.V., Myagkova I.N. Dynamics and energy of thermal and non-thermal components of the solar flare of January 20, 2005 according to the data of hard electromagnetic radiation detectors onboard the CORONAS-F satellite // Letters to the Astron. Journal. 2010. Vol.36, N4, pp.292 − 303.

Flux of the particles in the heliosphere at quiet Sun

In order to determine possible sources of particles of suprathermal energy (0,03-10 keV/nucleon) in the heliosphere the energy spectra of the ions C, O and Fe, relative content of the ions and energy relations of the ratios Fe/O and C/O according to the data of the ACE and the WIND spacecrafts were studied during the quiet periods of the 23rd solar activity cycle (1996-2010). It is shown that the fluxes of the studied particles during the quiet periods are separated into three types which differ by the shape of the energy spectra of C, O and Fe and relation of the values of relative content of the ions Fe/O and C/O to the energy. Fluxes of these types are originated from: the weak impulse flares, accelerated ions of the solar corona, high-energy tail of the SW particles. Distributions of the values of relative content of all studied ions are calculated. Difference between the histograms of the distributions of Fe/O, Fe/C and Fe/CNO are determined by the value of the first ionization potential (FIP) of the analyzed ions.
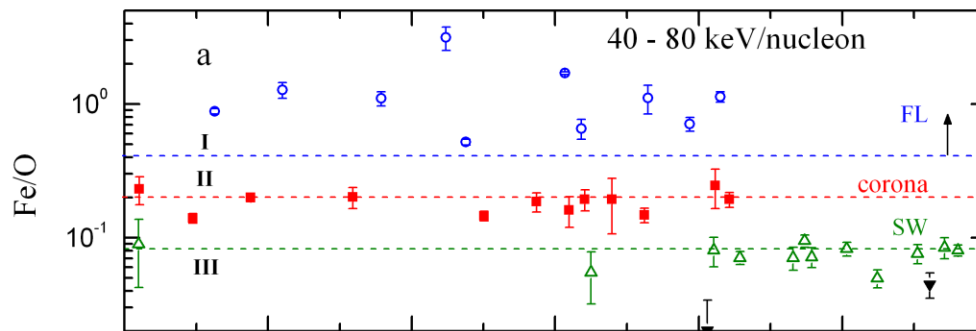
Fig. The values of Fe/O ratio with energy of 40-80 keV/nucleon during the quiet periods of the 23rd solar activity cycle. Line I corresponds to the average content of the ions in the impulse SCR flares. Lines II and III show the average content of the ions in the corona and the SW. Data for the periods of the group I are presented by blue circles, group II – red squares and group III – green triangles.

2. *Zeldovich M.A., Ishkov V.N., Logachev Yu.I., Kechkemeti K.* Ion content of the low-energy particles flux during the quiet periods of the solar activity at the distance of 1 a.u. // Izv. RAN, ser. Phys., 2011, vol. 75, N6, pp. 825-827.
3. *Zeldovich M.A., Logachev Yu.I., Surova G.M.* Energy spectra and relative content of the ions C, O and Fe at the distance of 1 a.u. For the quiet Sun // Astron. J., 2011, Vol.88, N4, pp. 409-416
4. *Ishkov V.N., Zeldovich M.A., Kecskeméty K., Logachev Yu.I.* Relative ion Fe, C and O abundances in quiet time particle fluxes in the 23 SC // Advances in Space Research, 2011, v. 46, p. 1433-1438

Characteristics of the SCR events

Statistical analysis of the phase of solar events decrease during the last three solar activity cycles is made on the basis of the database of the protons, electrons and alfa-particles developed basing on the results of the IMP-8, SOHO, ACE and «Helios-1, -2» spacecrafts within the particles rigidity range (R) from 0.1 up to 500 MV. The studied complex of the relations between the characteristic time of decrease (τ) and particles' rigidity (R) allows to make a conclusion about unavailable united dependence τ(R) and therefore, unavailable model interpretation within the wide range of rigidity. It is shown that exponential decrease of the particle flux which appears at similar integral properties of the environment characterizes homogeneity and quasi-stationary space in a near-Sun sector. The most common sectors of homogeneous space are of 15° size, often they can be of 45°, more seldom 90°, in exclusive cases - 180° and extremely rare – 360° (whole near-Sun space). Constancy of τ for the consequent events can be observed only for one sort of the particles, and it proves that in the corresponding sectors only high-frequency, responsible for the electrons' scattering, or low-frequency, responsible for the protons' scattering, parts of the magnetic field fluctuation spectrum are stable.

1.   *Daibog E.I., Kechkemeti K., Logachev Yu.I., Surova G.M.* Rigidity dependence of the characteristic time of decrease and free path for the SCR events // Space Res., 2010, Vol. 48, N6, pp. 516-523
2.   *Kecskeméty K., Yu.I. Logachev, M.A. Zeldovich, and J.Kóta* Modulation of the Galactic Low-Energy Proton Spectrum in the Inner Heliosphere // Astrophys. J., 2011, v. 738, № 2, p.173-182.

Solar cosmic rays particles spectrum

A new united form for description of the energy spectrum of the SCR particles within the 1.5 wider range (0.1÷1000 MeV/nucleon), consisted of two power parts separated with a knee is offered.
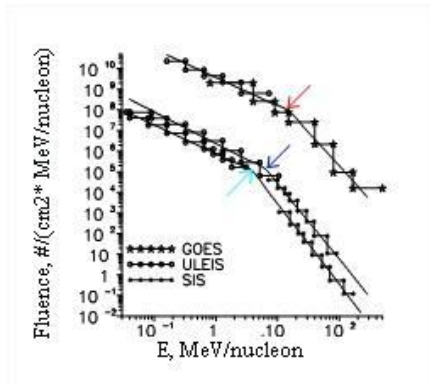

Fig. Logarithmically averaged fluxes of the fluences of 28 SCR events and approximating spectra for the protons, oxygen and iron (from the top to the low). The arrows show the point of the knee.

Nymmik R.A. The knees in the large-scale spectra of the protons and heavy ions of SCR: presentation, parameters and regularities. Izv. RAN, ser. Phys, Vol.75, N6, pp. 828-830, 2011.

Extremely high SCR fluxes

Basing on the results of the measuring the historical SCR fluxes by means of the analysis of radioactive isotopes content in the Greenland ice the function of distribution of the values of the extremely high proton fluxes in the individual SCR events is distributed for one order of magnitude to the extremely small probability direction.
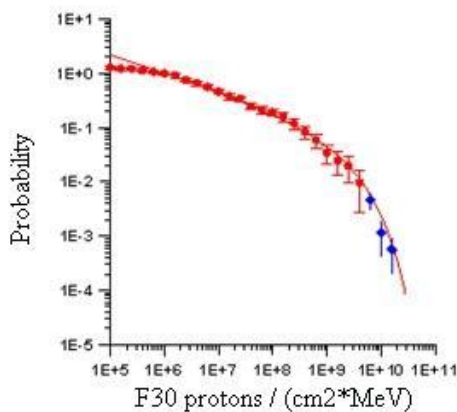

Fig. Distribution of the SCR events with proton fluence with energy of >30 MeV and flux $F30>10^6$ cm^2.

Dots − experimental data according to the SCs measurements;

diamonds − experimental data calculated by the author according to the isotopes' data of the Greenland ice;

line − distribution function used by the author in his numerous studies.

Nymmik R.A. Some problems with developing a standard for determining solar energetic particle fluxes // Advances in Space Research, vol.47, p. 622-628, 2011.

III.   *Theoretical models of electromagnetic processes in space*

Planets' magnetospheres basing on the paraboloid model

Important characteristics of the structure and dynamics of the magnetospheres of the Solar system planets were obtained during the studies based on the developed general (paraboloid) model of the planet's magnetosphere and according to the data of the scientific experiments in the Earth's

magnetosphere and the last space missions to the planets of the Solar system: Galileo (Jupiter), Cassini (Saturn) and Messenger (Mercury) and the data about the structure of the auroras observed by the space telescope (ST) Hubble in the upper atmosphere of the giant planets Jupiter and Saturn.

UV photos of the Saturn's auroras obtained by the ST Hubble were projected to the magnetosphere within the frames of the paraboloid model. It is shown that low-latitude border of the aurora is associated with interchangeable instability and the high-latitude one – with a shift of azimuth speed on the border between the opened and closed lines.

Fig. The structure of the power lines within the section "midday-midnight" in the Saturn's magnetosphere.
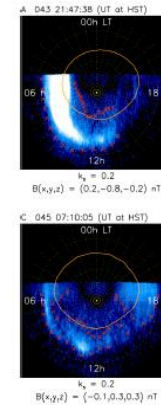

Fig. Oval of the Saturn's aurora obtained by the ST Hubble and high-latitude border of the aurora calculated according to the model.

1. *Belenkaya, E. S., Alexeev, I. I., Blokhina, M. S., Bunce, E. J., Cowley, S. W. H., Nichols, J. D., Kalegaev, V. V., Petrov, V. G., and Provan, G.* IMF dependence of Saturn's auroras: modelling study of HST and Cassini data from 12–15 February 2008 // Ann. Geophys., 28, 1559-1570, doi:10.5194/angeo-28-1559-2010, 2010.
2. *Igor I. Alexeev et al.* Mercury's magnetospheric magnetic field after the first two MESSENGER flybys // ICARUS Volume: 209 Issue: 1 Special Issue: SI Pages: 23-39 DOI: 10.1016/j.icarus.2010.01.024
3. *Belenkaya, E. S., Cowley, S. W. H., Nichols, J. D., Blokhina, M. S., and Kalegaev, V. V.* Magnetospheric mapping of the dayside UV auroral oval at Saturn using simultaneous HST images, Cassini IMF data, and a global magnetic field model // Ann. Geophys., 29, 1233-1246, doi:10.5194/angeo-29-1233-2011, 2011.

Model of the Mercury's magnetosphere

A global model of the Mercury's magnetosphere is developed taking into consideration multiple sub-storm disturbances and turbulence in the tail, accompanied with generation of vortex electrical and magnetic fields in the current layer of the tail of the magnetosphere. It is shown that the most efficient mechanisms of acceleration in the Mercury's magnetosphere are scattering of the particles on the plasma turbulence and scattering as a result of numerous dipolization during the sub-storm disturbances (which appear much more often than on the Earth and are significantly shorter). The upper limit of the accelerated particles energy is evaluated.
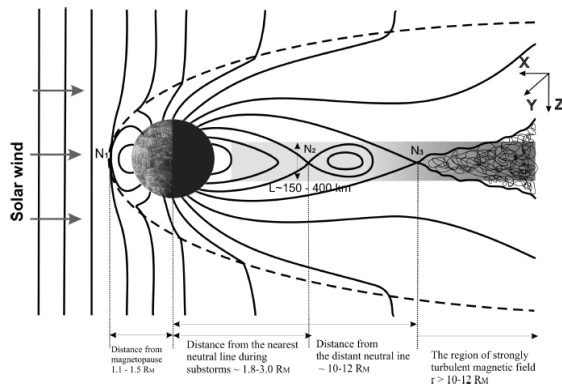
Fig. Schematic illustration of the Mercury's magnetosphere, washed by the SW. The most important magnetospheric regions and their distance from the center of the planet are specified.

Zelenyi L.M., A.G. Korgov, H.V. Malova, V.Yu. Popov, A.V. Artemyev and D.C. Delcourt, Charged particle acceleration in the Hermean magnetosphere: the role of dipolarizations, plasma turbulence and induction electric fields // in the book: Advances in Geosiences, A6, v19, p.p. 9-28, 2010

Current sheet of the Earth's magnetotail

Self-consistent theory of the anisotropic current balances realized in the plasma with non-Maxwell distribution of the particles over the rates in the case when plasma consists of cold electrons and two hot ion components with different temperatures is developed. Ion populations of the plasma are described within the frames of quasi-adiabatic approach, while electrons are described by the MHD approach. Approximate stationary solutions for the system of the Vlasov-Maxwell equations are obtained and parametrically analyzed. It is shown, that these solutions can describe different profiles of current sheets: from thin current structures with maximum current density in the neutral layer up to relatively "thick" current sheets with two or three maxima of the current density. It is also shown that electron component with anisotropic distribution dominates in the center of the current sheet and can support narrow central peak of the current density. Ion component dominates at the rims of the current sheet and determines its characteristic thickness. The results of numerical simulation for the two-temperature plasma (method of large particles) are in an agreement with experimental data obtained by the Cluster SCs.
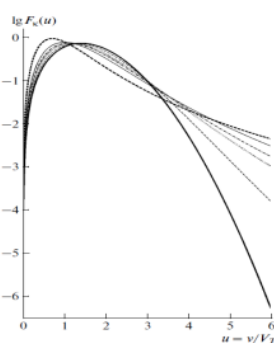

Fig. Comparison of the normalized distribution functions in the logarithmic coordinates:
$F_k(u)=u^2 A_k(1+u^2/(2k-3))^{-(k+1)}$
(so-called kappa-distribution; $u=v/V_T$,

V_T -- thermal speed). Maxwell distribution $F_m(u)=u^2 exp(u^2/2)$ is shown by thick solid line. Kappa-distributions are presented for $k=2,4,5,10$ (dashed and dash-dotted lines).
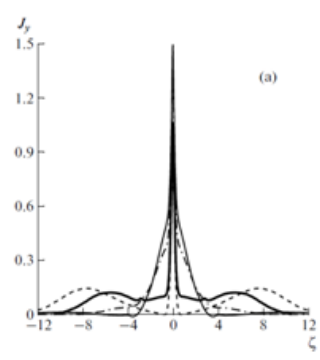

Fig. Profiles of the current density in the equilibrium current sheet in the case, when there are cold span and hot captured ions at different values of relative coefficient of the captured plasma density (minimum value corresponds to the profile, presented by thin solid line, maximum − by dashed line).

Malova H.V., L.M. Zeleny, O.V. Mingalev, I.V. Mingalev, V.Yu. Popov, A.V. Artemyev, A.A. Petrukovich, Current sheet in the collisionless non-Maxwell plasma: self-consistent theory, modeling and comparison with space experiments. // Phys. of plasma. Vol.36, N9, pp. 897-915, 2010

IV. *The studies of radiation environment and plasma processes in the near-Earth space*

Position of magnetopause

A class of quasi-stationary events, when long-term impact (several hours) of the interplanetary magnetic field directed along the flux of the SW plasma (quasi-radial field) results in the same long-term global widening of the magnetosphere was found. The size of the magnetosphere can be expanded up to 30% from the expected value. For the first time by means of the data of the THEMIS satellites it was experimentally proved that generation of the transition layer in the quasi-radial field is accompanied by abnormal low plasma pressure, which can be only 20% of the dynamic pressure of SW.
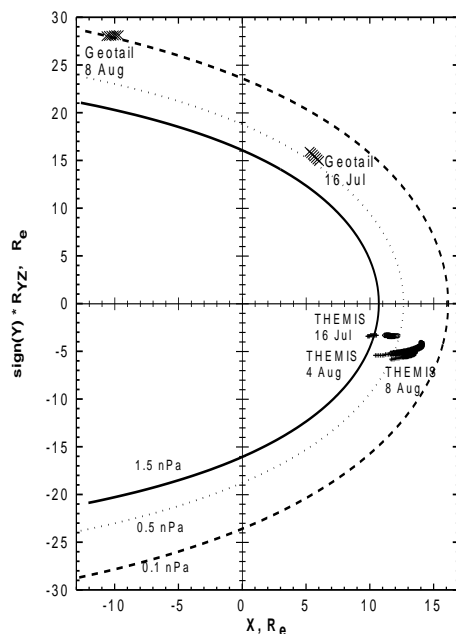

Fig. Location of 5 THEMIS and Geotail satellites and the borders of the magnetosphere (magnetopauses) calculated according to the model for three quasi-stationary events of 16.06.2007, 04.08.2007 and 08.08.2007. Expected position of magnetopause is calculated for the observed SW's pressure: 16.06 and 08.08 − 1.5 nPa (solid curve), 04.08 − 0.5 nPa (dots), and for the observed plasma pressure in the transition layer − 0.1 nPa (dashed line). The satellites were inside the magnetosphere during several hours, and it is in a good agreement with position of magnetopause, calculated for abnormal low pressure in the transition layer.

Suvorova, A. V., J.-H. Shue, A. V. Dmitriev, D. G. Sibeck, J. P. McFadden, H. Hasegawa, K. Ackerson, K. Jelinek, J. Safrankova, and Z. Nemecek Magnetopause expansions for quasi-radial interplanetary magnetic field: THEMIS and Geotail observations // J. Geophys. Res., 2010, 115, A10216, doi:10.1029/2010JA015404.

Model of SCR penetration to the high latitudes

Penetration of the solar cosmic rays (protons with energy from 240 keV up to >140 MeV and electrons with energy from 100 keV up to >300 keV) to the high latitudes for different levels of geomagnetic activity was studied basing on the data of five low-altitude POES spacecrafts. Developed elliptic model of SCR penetration describes such important effects, as shift of the cropping to the low latitudes at the night and evening sides as a result of magnetic effect of the tail's current and partial ring current, respectively. The model also allows to forecast absorption effect in the polar cap as a result of the increased ionization of the D-layer of the ionosphere by intensive flux of solar protons and electrons with energy >2.5 MeV and >100 keV, respectively.
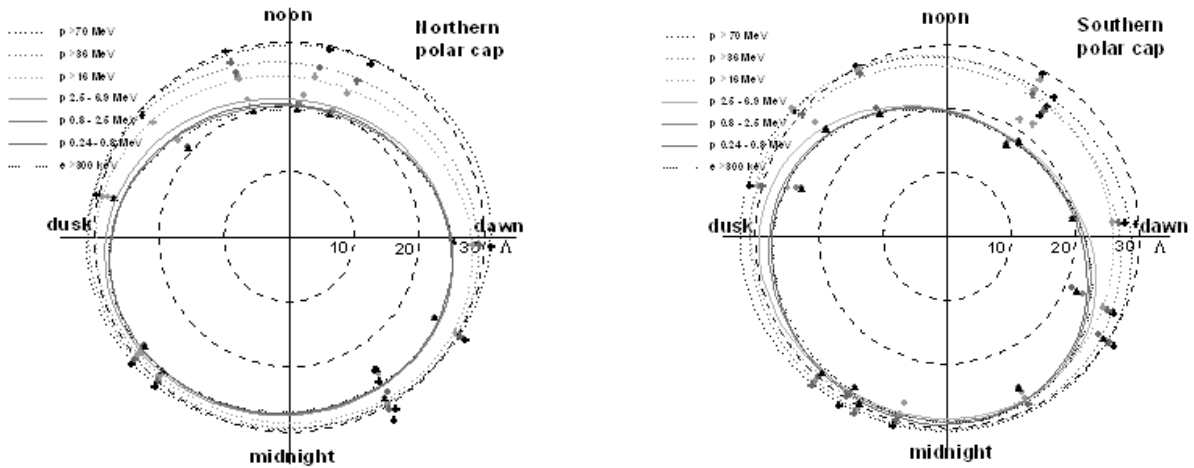
Fig. Cropping of SCR in the invariant system of coordinates during the magnetic storm at 17:00 14.12.2006 in the north (left) and south (right) hemispheres. It is seen that the latitude of the cropping decreases significantly and moves to the night and evening side.

Dmitriev, A. V., P. T. Jayachandran, and L.-C. Tsai Elliptical model of cutoff boundaries for the solar energetic particles measured by POES satellites in December 2006 // *J. Geophys. Res.*, 2010, 115, A12244, doi:10.1029/2010JA015380.

Boundaries of the SCR penetration into the Earth's magnetosphere

According to the data of simultaneous measurements onboard three SCs of the "COSMOS" series effect of hysteresis between the main phase and recovery phase of the strong magnetic storm in the position of the boundaries of the solar protons' penetration into the magnetosphere is studied. In the position of the boundaries distinct hysteresis is observed: at the recovery phase for the same local time the curve is several degrees higher. For the evening sector this difference at the same value of *Dst* at different phases of the storm can be up to 5°. It is explained by the development of asymmetric ring current at the main phase of the storm with predominant injection of the particles in the evening sector.
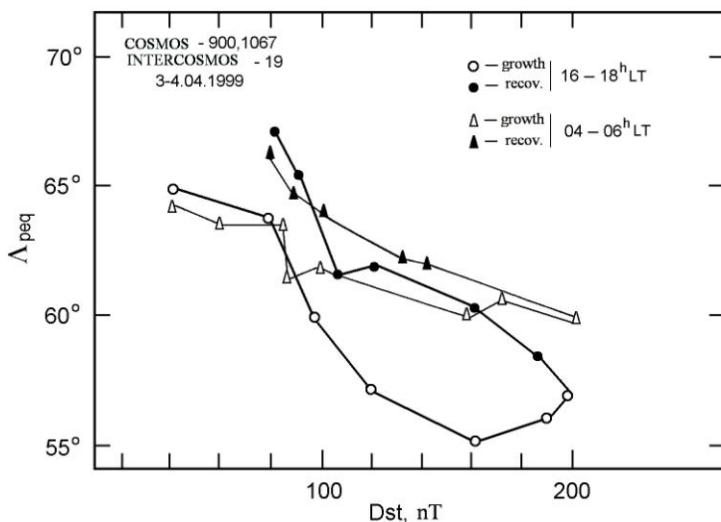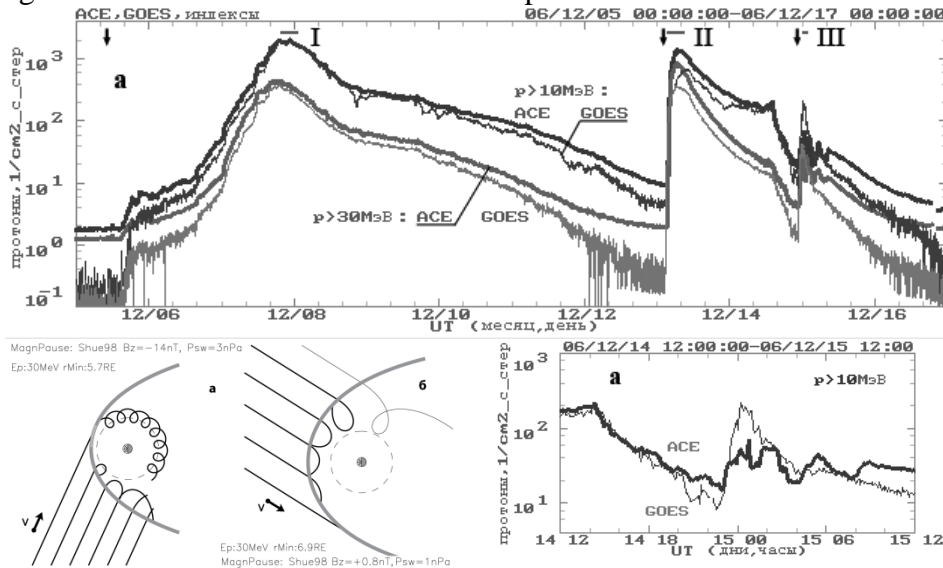

Fig. Position of the equatorial (Λ_{peq}) penetration boundaries for the SCR protons with energy over 1 MeV at different phases of the strong magnetic storm 3-4.04.1979. The dots are connected in time sequence. Light circles and triangles – evening and morning dots at the phase of the storm's development, respectively, dark – at the recovery phase.

Tverskaya L.V. Diagnostics of the magnetosphere according to the relativistic electrons of the outer belt and penetration of solar protons. // Geomag. And aeronomy.Vol.51 N1. pp.8-24. 2011

Penetration of solar energetic particles into the Earth's magnetosphere

Charged particles are accelerated in solar flares; they can go out to the heliosphere, fill it and penetrate into the Earth's magnetosphere, and the density of the penetrating radiation flux can be lower, equal or higher than out of the magnetosphere. In order to study the reasons of this effect a period when all three mentioned modes were observed under the comparable conditions was chosen. Variations of penetration mode were explained by means of relations of penetration efficiency and the angle of the particles' coming to the magnetopause (which is determined by the direction of the Interplanetary magnetic field and pitch-angular distribution of the particles for that moment) and magnetopause's characteristics (its shape and distance from the Earth). Qualitative agreement between the model and the experiment was shown.

Upper panel – particles flux for three events with different penetration modes are noted as I, II and III. Lower right panel – extended event III. Lower left panel – model schemes of the entry into the magnetosphere and depth of penetration for the events III (a) and II (b).

5. *Vlasova N.A., Pavlov N.N., Panasyuk M.I., et al.* Some peculiarities of solar cosmic rays penetration into the Earth's magnetosphere: December 05-17, 2006 // Space Res. 2011. Vol. 49. N6. pp. 500-515.
6. *Pavlov N.N.* The studies of the possibility for the penetration of high-energy solar particles into the Earth's atmosphere // 6th conf. "Plasma physics in the Solar system" (Abstracts), IKI RAS, 2011, p. 85.

Determination of the characteristics of the plasma ring surrounding the Earth

A database of the plasma pressure measured during the period from August 2007 till September 2010 by the THEMIS satellites is developed. The moments of the distribution functions of the ions and electrons recovered by two different instruments: ESA (ions with E=1.6 eV - 25 keV and electrons with E=2 eV - 32 keV) and SST (ions with E=25 keV - 6 MeV and electrons with E=25 - ~900 keV) were analyzed. For the first time the structure of statistically averaged distribution of the plasma pressure in the plasma ring surrounding the Earth at the geocentric distance from ~6 up to ~$10R_E$ is determined. It is shown that pressure distribution is close to the azimuth-symmetrical.
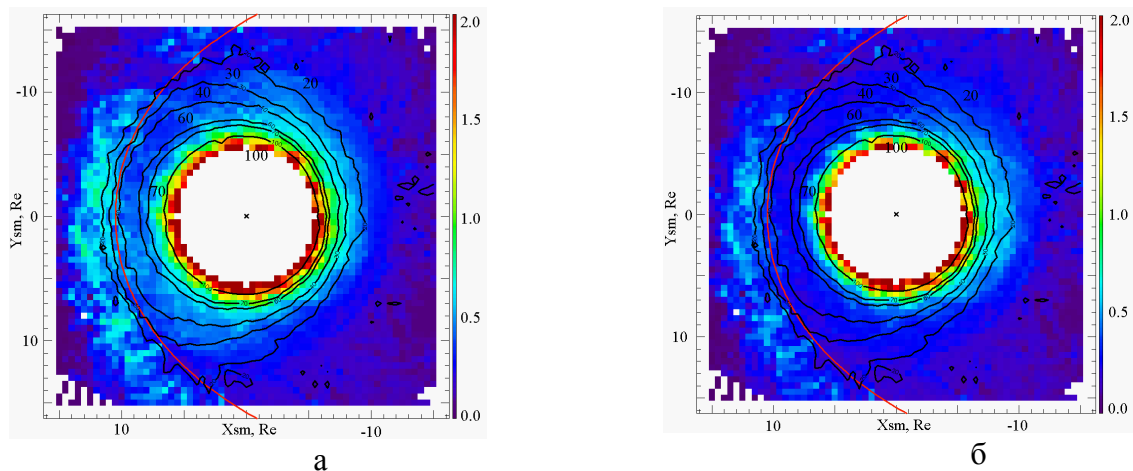
Fig. Distribution of $p_\perp$- average value of the component perpendicular to the magnetic field (a) and p_{II} — component along the magnetic field (b), components of the tensor of total plasma pressure (ions and electrons). Average position of magnetopause according to the model [Shue et al., 1998] and the levels of the constant value of the local magnetic field module are presented additionally.

Kirpichev I.P., Antonova E.E. Distribution of the plasma pressure in the equatorial plane of the Earth's magnetosphere at geocentric distances from 6 up to 10RE according to the data of the International project THEMIS // Geomag. And Aeronomy. Vol. 51 , N4, pp. 456-461, 2011.

Fluctuations of the plasma speed in the magentotail

The global statistically averaged distribution of diagonal components of the tensor of vortex diffusion in the plasma sheet of the Earth's magnetosphere during magnetically quiet period and during the magnetospheric sub-storm at the distances of up to 30 Earth's radii is obtained. Dependence of diagonal components of tensor of vortex diffusion at different geocentric distances in the plasma sheet of the Earth's magnetosphere was analyzed. Database from 5 satellites of the International project THEMIS was used. Amplitude of fluctuations and autocorrelation time were determined. Dependence of the coefficients from the phase of the sub-storm and geocentric distance was studied. The obtained results allow to explain localization of the beginning of the explosive phase of the magnetospheric sub-storm at relatively small geocentric distances $<10R_E$, where the level of turbulent fluctuations is not high and movement of plasma before the beginning of the explosive phase of the sub-storm is close to laminar.

Coefficient of quasi-diffusion across the plasma sheet, sheet's thickness and large-scale field "morning-evening" were measured simultaneously for the event of 12.09.2004, when the satellites of the CLUSTER project crossed the plasma sheet and the data from the radar SuperDARN were available, which allowed to evaluate the value of the field "morning-evening". The results of the analysis have shown that experimentally determined thickness of the turbulent plasma sheet is in a good agreement with theoretical predictions of the equilibrium turbulent plasma sheet made by Antonova and Ovchinnikov.
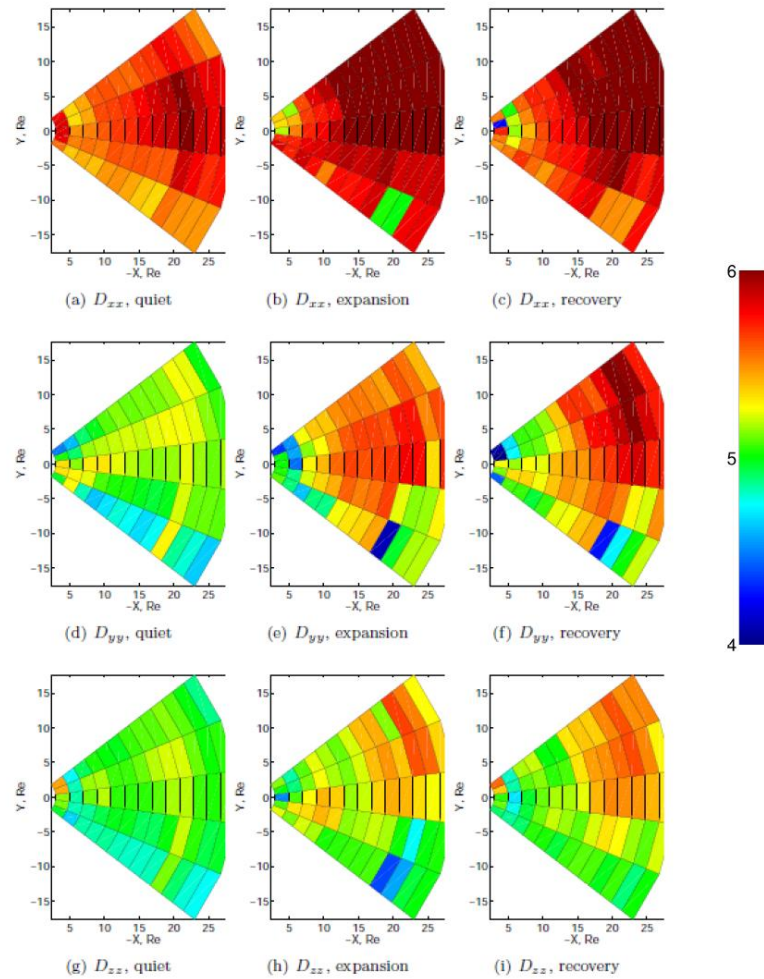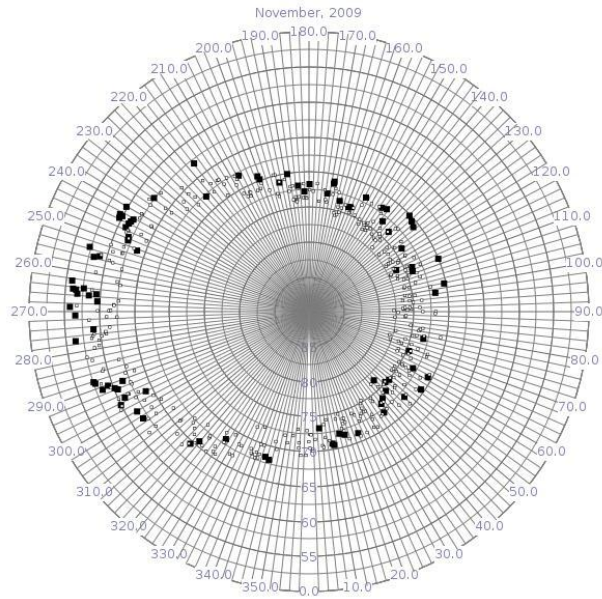
Fig. Global distribution of quasi-diffusion coefficients in the night magnetosphere.

Stepanova M., V. Pinto, J. A. Valdivia, and E. E. Antonova Spatial distribution of the eddy diffusion coefficients in the plasma sheet during quiet time and substorms from THEMIS satellite data // J. Geophys. Res. V. 116. A00I24. doi:10.1029/2010JA015887, 2011.

Stepanova M., E.E. Antonova Modeling of the turbulent plasma sheet during quiet geomagnetic conditions // Journal of Atmospheric and Solar-Terrestrial Physics. V. 73. Issue 13. p. 1636–1642. 2011.

The studies of the outer radiation belt of the Earth

Dynamics of the outer radiation belt of the Earth and position of its high-latitudinal boundary were studied basing on the data of simultaneous measurements conducted in November 2009 onboard the solar observatory CORONAS-FOTON and satellite METEOR-M 1. It is shown that during the period of low solar activity sharp (for several orders of magnitude) increases of the intensity of the outer radiation belt electrons were observed after coming of the high-speed fluxes of the SW to the Earth and it happened simultaneously with the increasing of the wave activity at high-latitudinal ground-based stations. The shape of the average position of the boundary at these altitudes is oval. Position and oval shape at the level of the ionosphere are determined by the characteristic features of the main magnetic field of the Earth: coordinates of the north magnetic pole and intensity of non-dipole harmonics of the interior field of the Earth.
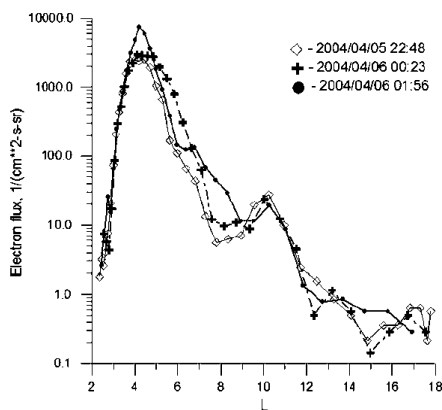
November, 2009

Fig. Intersections (in geographic coordinates) of the high-latitudinal boundary of the outer radiation belt by the satellites CORONAS-FOTON (Ee>200 keV, white signs) and METEOR-M1 (Ee>100 keV, black signs), detected during the simultaneous observation in November 2009.

Scatter of the points for each satellite is associated with effect of magnetospheric current systems, which are aimed to move the oval to the night region, but due to the daily rotation of the Earth influence on the different parts of the oval.
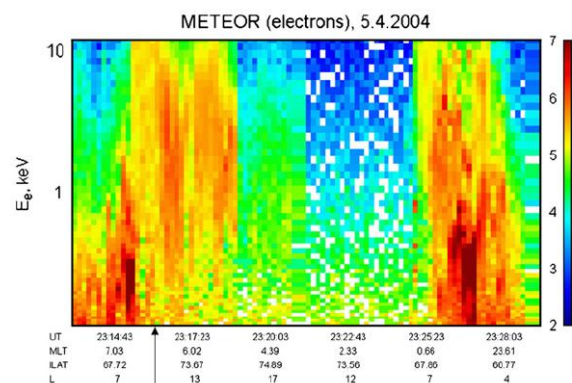
V.O. Barinova, A.V. Bogomolov, V.V. Kalegaev, I.N. Myagkova, M.I. Panasyuk, D.A. Parunakyan, M.O. Ryazantseva, L.I. Starostin Dynamics of the outer radiation belt of the Earth in November 2009 according to the data of the experiments onboard the satellites CORONAS-FOTON and METEOR-M1 // Vestnik MGU, ser.3, Physics. Astronomy. N6. pp. 122-127. 2011.

Quasi-stationary increases of the electron flux

Discovered earlier increases of high-energy electrons flux to the pole from the outer boundary of the outer radiation belt are analyzed. It is shown that the discovered increases are localized at the latitudes of the auroral oval and can be a result of generation of local magnetic traps for high-energy particles.

Fig. Dependence of the flux of electrons with energy of >300 keV, measured onboard the satellite CORONAS-F, on L (where L – McIlvine's parameter) for three consequent passes in the high-latitudinal region of the southern hemisphere on April 5-6, 2003.

Fig. Precipitation of auroral electrons measured onboard the satellite METEOR-3M on April 6, 2003 (an arrow shows the simultaneously measured increase's maximum to the pole from the outer radiation belt).
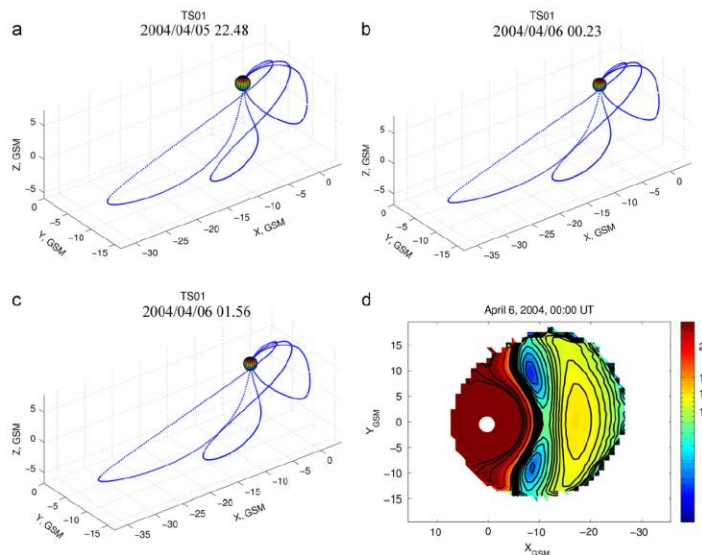
a TS01 2004/04/05 22.48

b TS01 2004/04/06 00.23

c TS01 2004/04/06 01.56

d April 6, 2004, 00:00 UT

Fig. The results of the projection of the increase of April 5-6, 2003 by means of the model Tsyganenko-2001 on the equatorial plane and position of the contours of magnetic field's minima in the equatorial plane Bmin=const

Antonova E.E., I.M. Myagkova, M.V. Stepanova, M.O. Riazantseva, I.L. Ovchinnikov, B.V. Mar'in, M.V. Karavaev Local particle traps in the high latitude magnetosphere and the acceleration of relativistic electrons // Journal of Atmospheric and Solar-Terrestrial Physics, V. 73, Issue 11-12, p. 1465–1471, 2011.

Ring current

Analysis of the experimental data on ring current (RC) resulted in numerical relationships which allow to predetermine radial profile of RC pressure during the magnetic storm basing on the ground-based magnetic data (D_{st}–variation) with high confidence.

1. It is estimated that at the main phase and at the recovery phase of the storm the functions describing the relation of the position of the pressure maximum in the evening sector and the current value of D_{st} differ essentially and at the recovery phase this relation is steeper. It is shown that power function describing relation between L_m and D_{st} at the main phase of the storms with characteristic value close to experimental values is resulted from the equation of drift motion of the RC's ions in the electrical and magnetic fields of geomagnetic trap. It draws out close to dipole character of the magnetic field near the maximum of RC and scale invariance of the particles' convection.
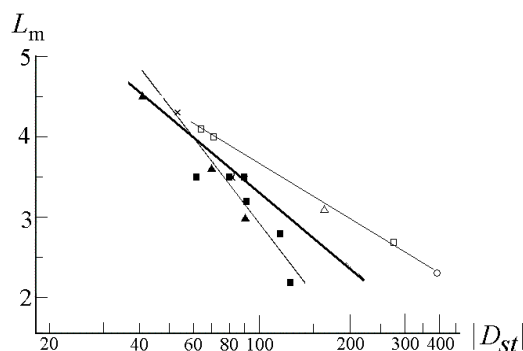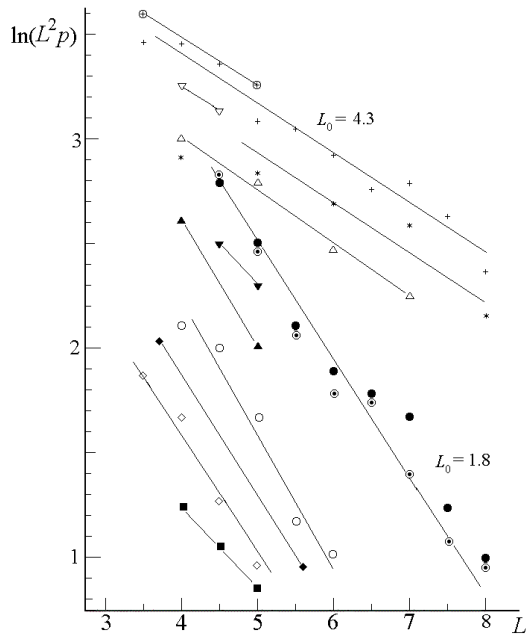

Fig. Root-mean-square exponential approximations of the position of pressure maximum basing on the RC data near the equatorial plane in the evening sector of MLT depending on the current value of D_{st} (nT). Light signs refer to the main phase, dark – to the phase of recovery of the storms. Thick line – approximation over all 16 points (without separation of the storms' phases).

2. It was shown that the shape of the outer boundary of the radial profile of the RC's pressure is described by the law $p(L) \approx aL^{-2}exp(-L/L_0)$ perfectly. This approximation corresponds to exponential increase of the total energy of the RC's particles at the given L-shell with decreasing of L. Characteristic value of $L_0 \sim 4$ at the main phase of the storm, and $L_0 \sim 2$ at the recovery phase. At the main phase of the storm parameter a anticorrelates to L_m, i.e. the deeper penetration of the RC must be provided by the higher pressure of hot plasma at the periphery of the trap. At the recovery phase of the storm the values of the RC's parameters a, L_m and L_0 are in a good agreement with the

current values of D_{st} parameter by the formula by Dessler-Parker-Skopke. It is shown that for the recovery phase of the storms the obtained relations $L_m(D_{st})$ are resulted from this formula. Effect of significant increase of the slope of the RC's outer boundary at the transit from the main phase to the recovery phase for the characteristic storms can be associated with the difference of the RC's asymmetry at these phases.

Fig. Radial profiles of the value $\ln(pL^2)$ at the outer boundary of the storm RC near the equatorial plane basing on the data obtained by different spacecrafts. Separate rows of dots (the same signs) are vertically spread for illustrative purposes.

3.   At the main phase of the storms the ratio of the plasma pressure to the magnetic field pressure in the RC's maximum is essentially independent on the power of the storm and L_m. It draws out opposition of the magnetic field of the Earth to the RC's expansion and gives evidence of the limited possibility of the RC's particles injection to the small L during the storms. At the recovery phase of the storms this value increases fast with increasing of L_m, drawing out the increase of the portion of the plasma within the total balance of pressures.

4. It is shown that maximum possible input of the RC into the storm D_{st}-variation is limited by the South-Atlantic anomaly of geomagnetic field and does not exceed 250–300 nT.

Kovtyukh A.S.   Radial profile of the pressure of the storm ring current as a function of Dst // Space Res. 2010. Vol. 48. N3. pp. 218-238.

Longitudinal asymmetry of proton fluxes

Dynamics of proton fluxes with energy of 30-80 keV and 80-240 keV, corresponding to the energy range of the RC's particles was studied basing on the data of three low-altitude polar satellites of the NOAA series (POES 15, 16, 17) during the geomagnetic storm of 21-22.I.2005. The characteristic features of longitudinal asymmetry of high-energy protons during the geomagnetic storm within two regions: higher and lower than the latitude of the isotropization boundary (quasi-captured and precipitated particles) were found. Constant longitudinal asymmetry of the precipitating particles fluxes was discovered. Asymmetry of quasi-captured particles fluxes is observed from the beginning of the storm till the late recovery phase. Maximum of the fluxes of precipitating particles averaged over the longitude is reached at the beginning phase of the storm.
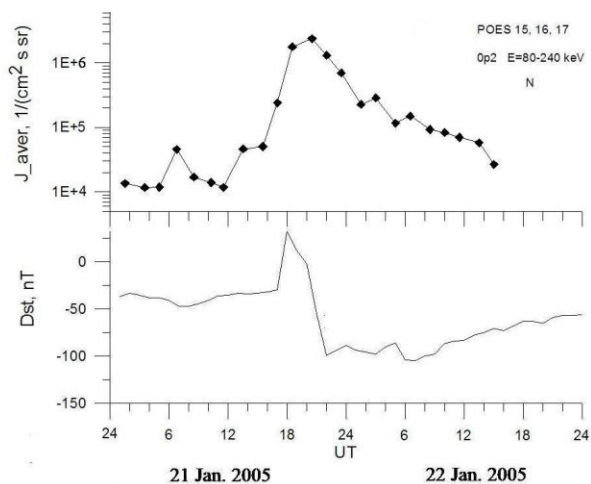
Fig. Temporal profiles of the maximum fluxes of the precipitating protons averaged over the longitude and of Dst-index 21-22.I.2005
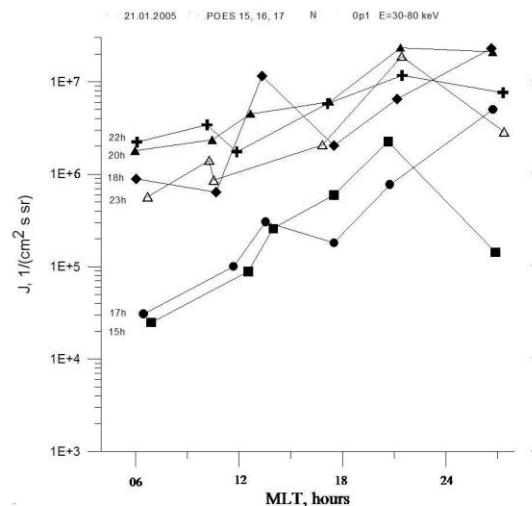
Fig. Longitudinal distribution of the maximum fluxes of the precipitating protons 21.I.2005.

Kalegaev V.V., Vlasova N.A., Some peculiarities of longitudinal distribution of proton fluxes at high latitudes // Advances in Space Research. 2011. V. 48. C. 2028-2035. doi: 10.1016/j.asr.2011.08.010.

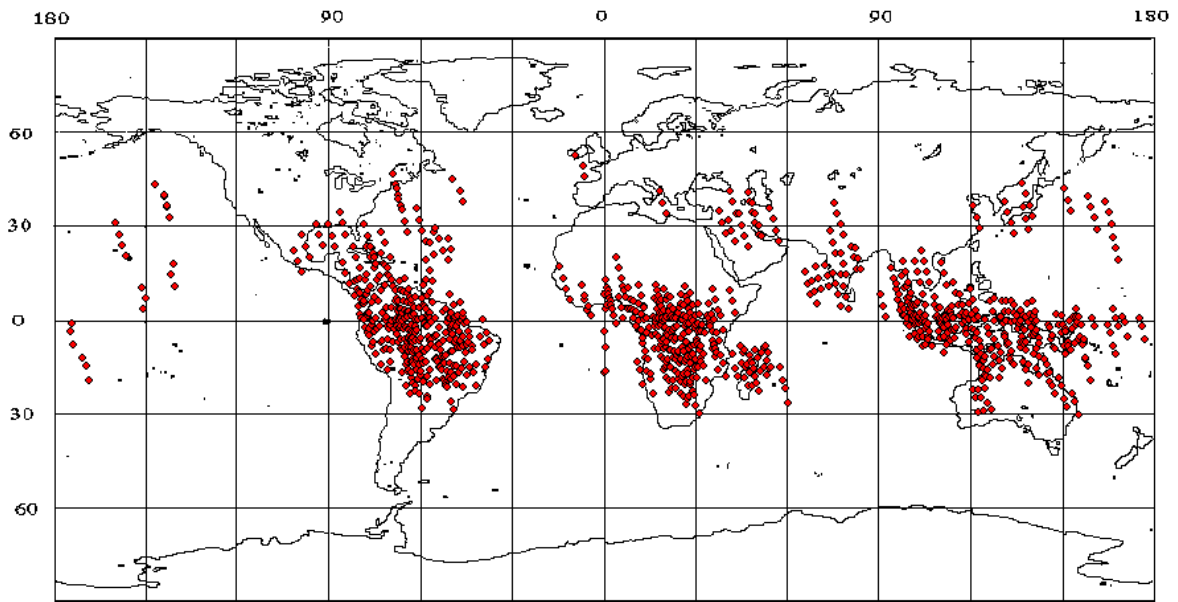### UV radiation of the upper atmosphere

Statistical analysis of the high-energy electron fluxes in the near-Earth space and of the intensity of the night atmosphere luminescence within the range of 300-400 nm has shown three regions of the increased intensity of UV radiation at low, middle and high latitudes. The obtained numerical evaluations of UV radiation intensity have shown that stable and quasi-stable fluxes of the precipitating electrons do not provide the observed intensity of UV radiation at low and middle latitudes. At the same time it is possible that UV radiation at high latitudes is resulted from the precipitating electrons. UV radiation at low latitudes I related from mesospheric atomic oxygen, which concentration increases essentially at the latitudes from 20° to 40°.

Panasyuk M.I., Bogomolov V.V., Garipov G.K., et al. Transient Luminous Event Phenomena and Energetic Particleы Impacting the Upper Atmosphere: Russian Space Experiment Programs // Journal Geophys. Res. 2010. V.115, A00E33, doi: 10.1029/2009JA014763.

Dmitriev A.V., H.-C. Yeh, M.I. Panasyuk, V.I. et al. Latitudinal profile of UV nightglow and electron precipitations // Planetary and Space Science. 2011. V.59, p. 733–740.

Nightglow of the Earth's atmosphere

For the first time the data obtained onboard the satellite "Universitetsky-Tatiana-2" allowed to separate not only the flashes generated directly above the lightnings but also the flashes far from the light (sometimes at the distance of thousands km from the lightning region) from the short-term (duration from parts of ms up to hundreds of ms) flashes of UV-radiation in the upper atmosphere (which were named transients). Series of flashes observed every minute at the trajectory of the satellite including its parts above the cloudless regions were registered for the first time. The last events are of particular interest because they are the evidence of excitation and further luminescence of the upper atmosphere in the vast regions neighbor to the lightning regions.

Fig. Distribution of the flashes of the series over the map.

1. *Vedenkin N.N., Garipov G.K., Klimenko I.I. Et al.* Atmospheric flashes within UV and IR ranges according to the data of the "Universitetsky-Tatiana-2" satellite // JETP. 2011. Vol. 140. pp. 900-910.
2. *Sadovnichy V.A., Panasyuk M.I., Yashin I.V. Et al.* The studies of the space environment onboard the satellites "Universitetsky-Tatiana" and "Universitetsky-Tatiana-2" // Astronom. Vestnik. 2011. Vol.45. N1. pp. 3-29.
3. *G.K. Garipov,B.A. Khrenov, P.A. Klimov et al.* Global Transients in ultraviolet and red-infrared ranges from data of the "Universitetsky-Tatiana-2" satellite // Archiv-astro. 2011.

V. Space dosimetry

Radiation conditions of the Moon

A method for calculation assessment of the radiation conditions on the Moon for the lunar expeditions is developed. The calculated flux of the particles of the primary (protons and nuclei of GCR and SCR) and secondary (protons and neutrons from the aluminum shield and lunar subsoil) radiation were used in order to evaluate yearly absorbed and equivalent average tissue radiation doses on the surface of the Moon and in the lunar subsoil.
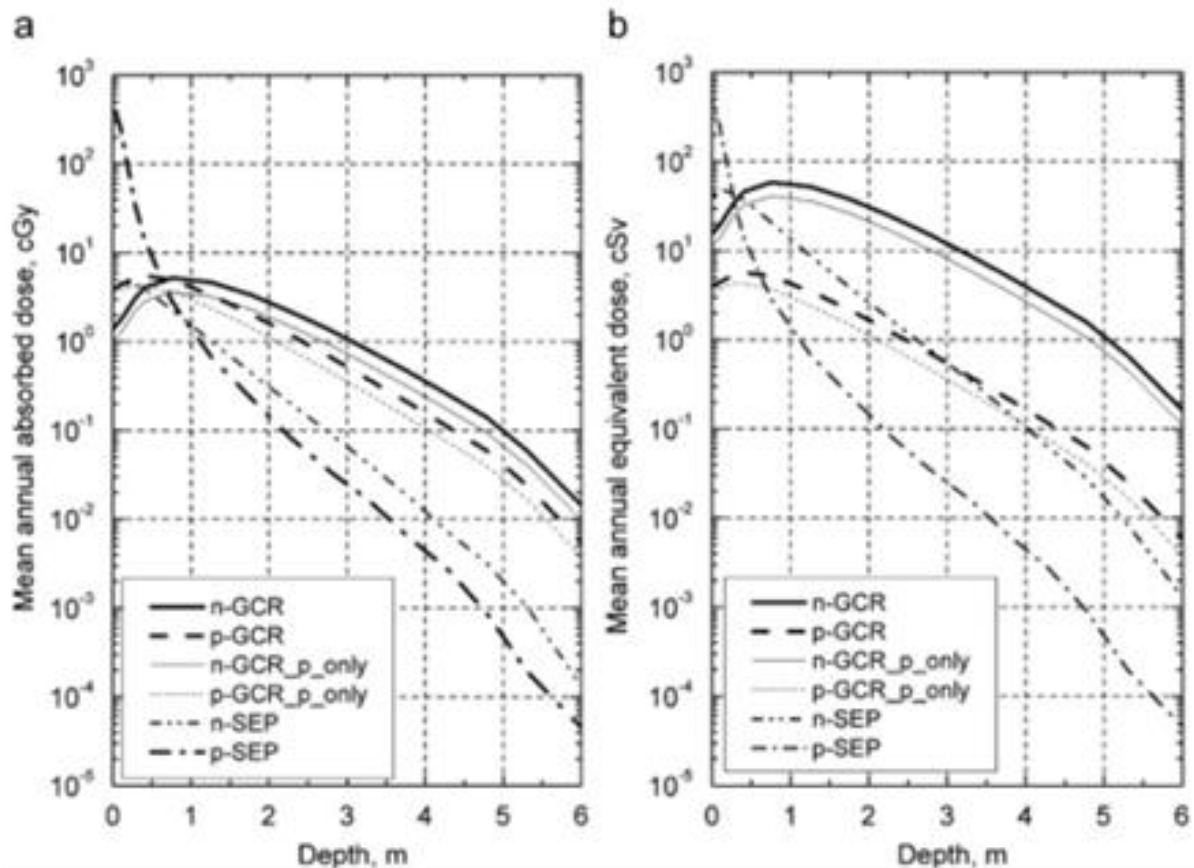

Fig. Inputs of the protons (p) and neutrons (n) into the absorbed (a) and equivalent (b) average tissue radiation doses depending on the depth of the lunar subsoil

Denisov A.N., N.V. Kuznetsov, R.A. Nymmik, M.I. Panasyuk, N.M. Sobolevsky Assessment of the radiation environment on the Moon // Acta Astronautica. 2011. V.68. C. 1440–1447.

Radiation conditions near the Jupiter

Radiation conditions of the planned space research mission to the Jupiter and its satellite Europe were studied. Spatial distribution of the fluxes of the Jovian radiation belts charged particles and radiation doses behind different protection near the Europe was simulated taking into account several factors and the most safe regions for the landing of the lander to the surface of the Europe and the orbits around it at the altitude of 100 km from the point of radiation influence are indicated.
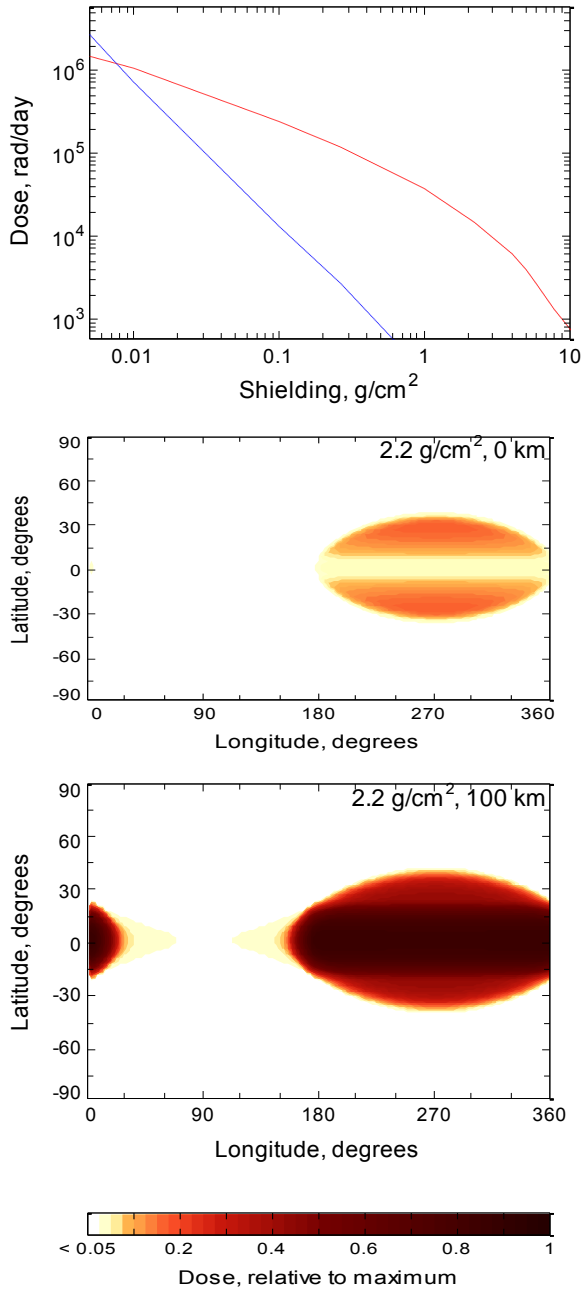
Fig. Upper panel – the radiation doses from the electrons (upper curve) and protons (lower curve) in the region of the Europe's orbit. Lower panel represents the spatial distribution of the doses behind the protection of 2.2 g/cm² Al on the surface of the Europe and at the altitude of 100 km.
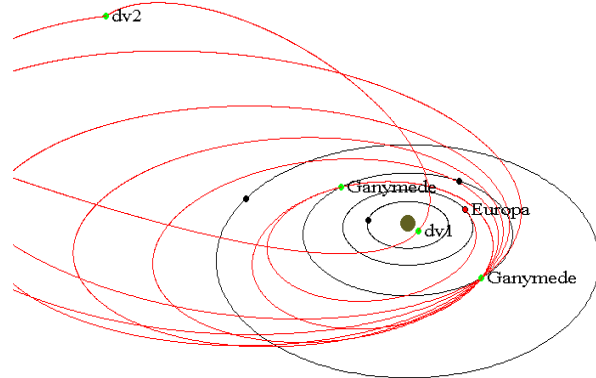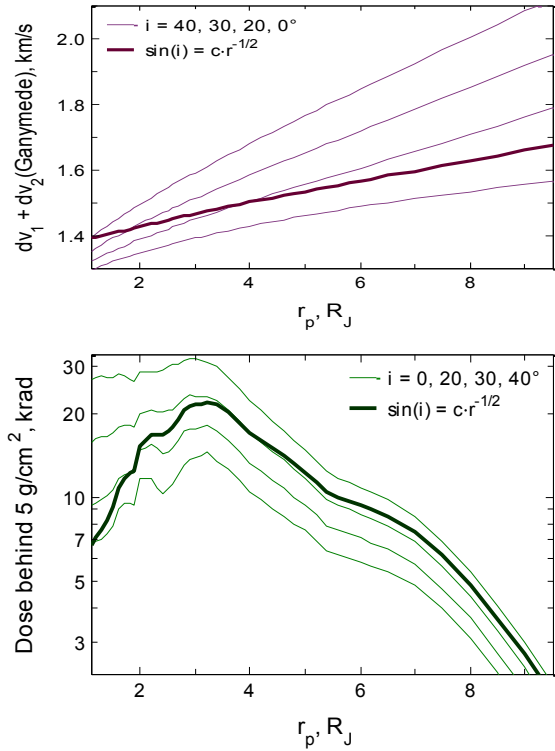
Fig. Upper panel – dependence of the summarized impulse $dv_1 + dv_2$ and dose behind the protection of 5 g/cm² during the 1st pass of the Jupiter from the radius of pericenter for several mentioned inclinations of the orbit (thin curves) and for the approximation of real dependence of inclination from pericenter radius (thick curves). Lower panel – an example of the optimum trajectory for gravitational manoeuvre in the Jovian system.

M. V. Podzolko, I. V. Getselev, Yu. I. Gubar, I. S. Veselovsky, A. A. Sukhanov, Charged particles on the Earth-Jupiter-Europa spacecraft trajectory // Advances in Space Research, 2011, v. 48, p. 651−660.